RSC Advances

PAPER

View Article Online
View Journal | View Issue

Cite this: *RSC Adv.*, 2024, **14**, 23273

Synthesis of star-shaped poly(lactide)s, poly(valerolactone)s and poly(caprolactone)s *via* ROP catalyzed by N-donor tin(II) cations and comparison of their wetting properties with linear analogues†

Miroslav Novák, *[a] Yaraslava Milasheuskaya,[b] Michael Srb,[b] Štěpán Podzimek,[a] Marek Bouška[c] and Roman Jambor[b]

In this study, we report the use of N-coordinated tin(II) cations $[L^1{\rightarrow}Sn(H_2O)][OTf]_2{\cdot}THF$ (**1**) and $[L^1{\rightarrow}SnCl][SnCl_3]$ (**2**) (L^1 = 1,2-(C$_5$H$_4$N-2-CH = N)$_2$CH$_2$CH$_2$) as efficient ROP catalysts, which, in combination with benzyl alcohol, afford well-defined linear poly(ε-caprolactone) (PCL) and poly(δ-valerolactones) (PVL) *via* an activated monomer mechanism (AMM). Thanks to the versatility of complexes **1** and **2** as catalysts, star-shaped PCL, PVL and PLA were also prepared using three-, four-, five- and six-functional alcohols. The number of arms was determined by SEC-MALS-Visco analysis. Spin-coated thin layers of linear and selected six-armed polymers were further studied in terms of their wettability to water. Attention was focused on the influence of the composition and structure of the polymers. Finally, to increase the hydrophobic properties of the studied polymers, stannaboroxines L^2(Ph)Sn[(OB-(C$_6$H$_4$-4-CF$_3$))$_2$O] and L^2(Ph)Sn[(OB-(C$_6$H$_4$-3,5-CF$_3$)$_2$)$_2$O] (L^2 = C$_6$H$_3$-2,6-(Me$_2$NCH$_2$)$_2$) were applied.

Received 13th May 2024
Accepted 14th July 2024

DOI: 10.1039/d4ra03515a

rsc.li/rsc-advances

Introduction

In past decades, linear aliphatic polyesters, such as poly(lactide) (PLA) or poly(ε-caprolactone) (PCL), have received great attention due to their biodegradable and biocompatible properties.[1] For this reason, they are nowadays a very suitable alternative to classic petroleum-based plastics and, in particular, poly(lactides) have found application in many areas such as building and packaging materials, electronic components, pharmacy and medicine.[2] Besides these applications, biodegradable polyesters are considered as relatively hydrophobic materials and for this reason they have found an attractive application in the preparation of non-fluorinated hydrophobic materials, *i.e.* water-repellent, self-cleaning materials or membranes in oil-water separation, *etc.*[3] The classification of the hydrophobic properties of materials is based on the measurement of the contact angle of water (WCA, θ), for example by the sessile drop method. The final wetting properties depend not only on the type of polymer and thus their surface energy, but also on the topography of the studied substrate, which is associated with the fabrication method. In the case of PCL, the most hydrophobic materials were prepared by electrospinning, when a series of nanofibers, meshes, scaffold, sheets and tissues was obtained.[3b–h] These materials showed WCAs in the range of 113–136°.[3b–h] The electrospinning method has also become an excellent way to manufacture hydrophobic and superhydrophobic PLA-based materials. It has been reported that PLA nanofibers prepared in this way show WCA = 152° and the application of these fibers on a cellulosic cotton substrate provides a very effective membrane for water-oil separation with an efficiency of 99.16%.[3m] A similar results on hydrophobic electrospun-made PLA membranes and fibers was demonstrated by Zhang and Opaprakasit, who reported materials with WCAs of 133° and 110°, respectively.[3n,o] On the other hand, the electrospinning process is more complex and not all PLA-based materials show a hydrophobic character. Recently, PLA fibers with a flat and smooth surface have been produced, resulting in a WCA of 86.7°.[3k] Besides the electrospinning process, a simple approach based on the solvent casting method of dioxane solution of PLA were implemented to obtain superhydrophobic PLA surfaces.[3i] While the film obtained only from dioxane solution exhibited WCA = 66.6°, the precipitation of PLA from dioxane-water or dioxane-ethanol solutions in the combination with the gelation in air led to a WCA higher than 150°.[3i]

[a]*Institute of Chemistry and Technology of Macromolecular Materials, Faculty of Chemical Technology, University of Pardubice, Studentská 573, 53210 Pardubice, Czech Republic. E-mail: miroslav.novak@upce.cz*

[b]*Department of General and Inorganic Chemistry, Faculty of Chemical Technology, University of Pardubice, Studentská 573, 53210 Pardubice, Czech Republic*

[c]*Department of Graphic Arts and Photophysics, Faculty of Chemical Technology, University of Pardubice, Studentská 573, 53210 Pardubice, Czech Republic*

† Electronic supplementary information (ESI) available. See DOI: https://doi.org/10.1039/d3ra03515a

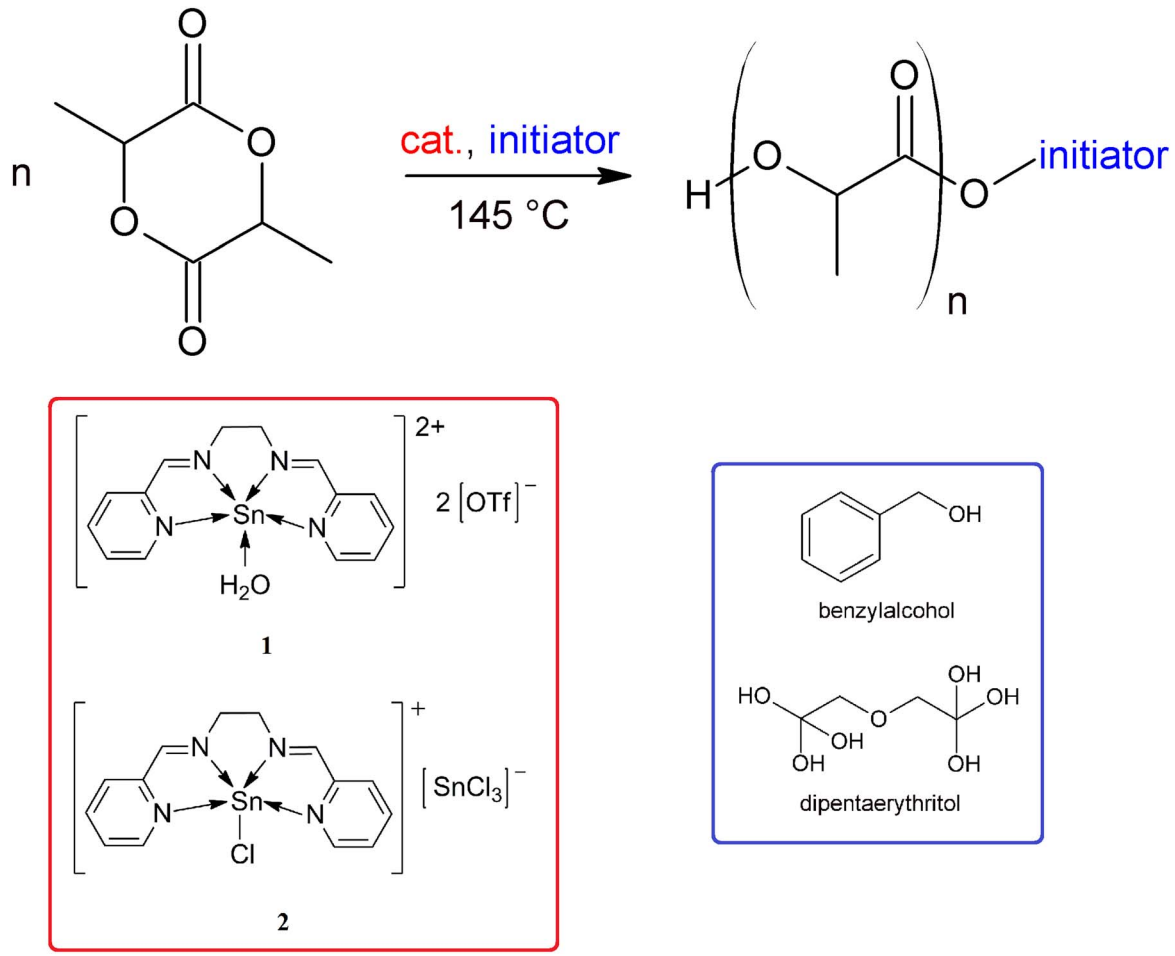

Scheme 1 ROP of L-lactide catalysed by complexes **1** and **2**.

The hydrophobic properties of biodegradable polymers could be influenced not only by their surface energy and topography, but also by the structure of the polymer. In particular, star-shaped polymers have become the object of great interest due to their unique structure and topological properties, which cannot be achieved in the case of linear polymers.[4] These polymers are composed of several linear arms radiating from central core, which causes a high proportion of chain ends and a higher concentration of functional groups than in their linear analogues of the same molar mass.

Two possible polymerization techniques are applicable to produce star-shaped polyesters. The first one is based on polycondensation of dicarboxylic acids with polyalcohols, which, however, yield polymers with $M_n < 4700$ g mol^{-1}.[5] On the other, an incorporation of catalysts based on *p*-toluenesulfonic acid[6] or triphenylphosphonium trifluoromethanesulfonate[7] led to the isolation PLAs with M_n up to 67 000 g mol^{-1}. The second and more widespread method is the ring-opening polymerization (ROP) of cyclic esters operating by the coordination insertion or activated monomer mechanism.[8] This method is popular mainly due to the excellent control, robustness, versatility, and simple reaction setup. Besides the monomer, the key components of the ROP are initiator and catalyst.

Almost all reports used $Sn(Oct)_2$ to catalysed the formation star-shaped polyesters.[9] $Sn(Oct)_2$, operating *via* coordination-insertion mechanism, is a very efficient catalyst and it has low toxicity as reported by the Food and Drug Administration (FDA, USA) for biomedical applications.[10] For the synthesis of star-shaped polymer, the polymerization of L-LA in the bulk with $Sn(Oct)_2$ as catalyst was usually carried out at 130 °C.[11] Further, other tin compounds as spirocyclic tin initiators based on tin-substituted polyethylene ethoxylate,[12] cyclic stannoxane,[13] tin acetylacetonate,[14] tetraphenyltin[15] were have also been used with success. Besides tin compounds, other catalysts such as calcium hydride,[16] potassium hexamethyldisilazide[17] and bismuth(III) acetate[18] were also employed. Further, more biologically friendly aluminium salen and salan,[19,20] zinc amino-, thiophenolate or zinc amido-oxazolinate[21] and diiminate complex[22] extended the range of metal mediators for the synthesis of star-shaped polyesters. In addition, Lewis acid catalysts based on tin and aluminum allowed control of polymerization and provided polymer stars with variable tactics.[23]

Recently, we reported the utilization of N-coordinated tin(II) cations $[L^1 \rightarrow Sn(H_2O)][OTf]_2 \cdot THF$ (**1**) and $[L^1 \rightarrow SnCl][SnCl_3]$ (**2**) (L^1 = 1,2-$(C_5H_4N\text{-}2\text{-}CH=N)_2CH_2CH_2$) as the examples of Lewis acidic tin(II) catalysts in the ROP of L-LA (see Scheme 1).[24] It has

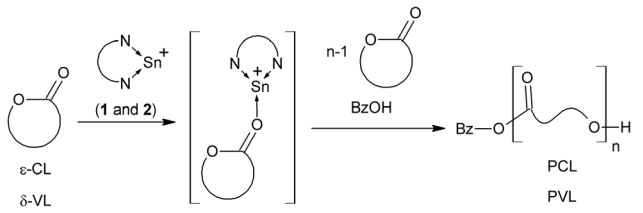

Scheme 2 ROP of δ-VL and ε-CL catalysed by **1** and **2** using BzOH as initiator.

been demonstrated that polymerization operates *via* activated monomer mechanism and the kinetic studies indicated a pseudo-first order reaction, and thus a good control over the polymerization.

Therefore, we set out the study to prove that **1** and **2** are the universal catalysts for ROP of other monomers, δ-valerolactone (δ-VL) and ε-caprolactone (ε-CL), to prepare linear biodegradable polyesters.

In addition, the formation of activated monomer also opens the possibility to use different polyalcohols instead of benzylalcohol for the synthesis of star-shaped polymers. Thus, the application of **1** and **2** in the synthesis of star-shaped polyesters poly(L-lactide)s, poly(δ-valerolactone)s and poly(ε-caprolactone)s using glycerol, trimethylolpropane, triethanolamine, pentaerythritol, xylitol, *myo*-inositol, D-sorbitol and dipentaerythritol as different polyalcohols is another goal of this study. These experiments provided three-, four-, five- and six-armed stars. The linear and star-shaped polyesters were characterized by SEC-MALS-Visco analysis.

Further, since the linear PLA showed good water-repellent properties, we tested selected linear and star-shaped polyesters as hydrophobic materials. Due to the good solubility and film-forming properties, we prepared thin layers of selected linear and star-shaped polyesters by spin-coating method. The spin-coating method led to the preparation of uniform thin-layers, in which it was possible to study the hydrophobic properties only based on their composition and structure. Finally, the effect of stannaboroxines $L^2(Ph)Sn[(OB\text{-}(C_6H_4\text{-}4\text{-}CF_3))_2O]$ and $L^2(Ph)Sn[(OB\text{-}(C_6H_4\text{-}3,5\text{-}CF_3)_2)_2O]$ ($L^2 = C_6H_3\text{-}2,6\text{-}(Me_2NCH_2)_2$)[25a] on the hydrophobic properties of thin layers of polyesters is also discussed. Both compounds with six-membered SnB_2O_3 central core were selected as properly soluble and good film-forming compounds,[25a] that structurally resemble polymer N-Boroxine-PDMS with six-membered B_3O_3 central core. This polymer in the combination with SiO_2 nanoparticles was recently published as hydrophobic material with WCA = 160.8°.[26]

Results and discussion

Synthesis and characterization of linear polyesters PVL and PCL

Recently, compounds **1** and **2** proved to be effective catalysts in ROP of L-LA. The computational study confirmed that ROP operates *via* activated monomer mechanism. The kinetic studies indicated a pseudo-first order reaction with a similar polymerization rate ($k = 5.44 \times 10^{-2}$ min^{-1} for **1** and $k = 4.93 \times 10^{-2}$ min^{-1} for **2**), and thus a good control over the polymerization. Complexes **1** and **2** are also universal in the ROP of other cyclic esters, which was demonstrated by the preparation of linear PVL and PCL (see Scheme 2).

All polymerization tests were performed in bulk at 145 °C. δ-VL and ε-CL was purified by the distillation over CaH_2 to avoid data fluctuations due to the variation of impurities in the technical grade monomers. The polymerization reactions were carried out at molar ratios of [catalyst] : [monomer] = 1 : 50, 1 : 100, 1 : 200 and 1 : 500. In all reactions, benzyl alcohol (BzOH) was added as an initiator in a molar ratio of 1 : 1 compared to the catalyst. The conversion a kinetics of the polymerization experiments was monitored by the ^{1}H NMR spectroscopy and showed a similar process as in the case of PLA. The data thus demonstrated not only the same process, but also the same activated monomer mechanism. All isolated polymers were further characterized by the combined SEC-MALS-Visco analysis with the aim to determine the number-average molar mass (M_n) and dispersity ($Đ$). Results on polymerization tests are summarized in Table 1.

As in the case of polymerization of L-LA,[24] the different charge of the tin atom in **1** and **2** does not have significant influence on the polymerization rate of δ-VL a ε-CL, since both catalysts **1** and **2** are very active and almost complete conversion of monomers (for molar ratio [catalyst] : [monomer] = 1 : 50, 1 : 100 and 1 : 200) was occurred after 1 hour. However, for a molar ratio of 1 : 500, the catalytic activity of **1** and **2** decreases, when after 1 hour the conversion was in the range of 65–78%. Furthermore, the isolated PVLs showed macromolecular parameters with only small deviations independently of the catalyst used. The determined $M_{n,SEC}$ should correspond to $M_{n,th}$ within the controlled living ROP, which is given by the equation $M_{n,th}$ = [monomer] : [cat] × M(monomer) × conversion + M(alcohol). In our case, this condition is met, for both catalysts **1** and **2**, especially by the molar ratio [cat] : [monomer] = 1 : 50 (and for PCL also 1 : 100 and 1 : 200). The prepared PVLs and PCL (in the molar ratio of 1 : 100, 1 : 200 and 1 : 500 for PVL and 1 : 500 for PCL) show lower $M_{n,SEC}$ than the theoretical ones, which can be caused by the traces of water in monomer and deactivation of catalyst (especially in a higher loading of monomer) resulting in the inhibition of the polymerization. So, **1** and **2** produces PVLs with M_n in the range of 4000–11 600 g mol^{-1} for **1** and 4100–16 500 g mol^{-1} for **2** and 5700–24 700 g mol^{-1} for **1** and 5900–16 500 g mol^{-1} for **2** in the case of PCL. The dispersity $Đ$ (1.46–1.60 for PVLs and 1.42–1.58 for PCLs) demonstrates a relatively uniform nature of polymers.

Based on these data, it can be concluded that the ROP of δ-VL and ε-CL catalysed by complexes **1** and **2** is relatively well controlled and the character of polymerization is very similar to L-LA polymerization catalysed by same complexes.[24]

Synthesis and characterization of star-shaped polyesters PLA, PVL and PCL

Compounds **1** and **2** showed the ability to polymerize L-LA, δ-VL and ε-CL *via* activated monomer mechanism providing linear

Table 1 ROP of δ-VL and ε-CL catalysed by **1** and **2** using BzOH as initiator

Entry	Catalyst	[cat]:[BzOH]:[δ-VL]	Conv[a] [%]	$M_{n,th}$[b] [g mol^{-1}]	$M_{n,SEC}$[c] [g mol^{-1}]	$Đ$
1	**1**	1 : 1 : 50	99	5100	4000	1.55
2	**1**	1 : 1 : 100	99	10 000	5900	1.55
3	**1**	1 : 1 : 200	98	19 700	13 100	1.60
4	**1**	1 : 1 : 500	65	32 600	11 600	1.46
5	**2**	1 : 1 : 50	98	5000	4100	1.51
6	**2**	1 : 1 : 100	99	10 000	7200	1.53
7	**2**	1 : 1 : 200	96	19 300	15 800	1.59
8	**2**	1 : 1 : 500	68	34 100	16 500	1.48
Entry	Catalyst	[cat]:[BzOH]:[ε-CL]	Conv[a] [%]	$M_{n,th}$[b] [g mol^{-1}]	$M_{n,SEC}$[c] [g mol^{-1}]	$Đ$
9	**1**	1 : 1 : 50	97	5600	5700	1.45
10	**1**	1 : 1 : 100	98	11 200	8000	1.55
11	**1**	1 : 1 : 200	99	22 700	15 100	1.58
12	**1**	1 : 1 : 500	78	44 600	24 700	1.46
13	**2**	1 : 1 : 50	98	5700	5900	1.42
14	**2**	1 : 1 : 100	98	11 200	9700	1.47
15	**2**	1 : 1 : 200	99	22 700	20 400	1.53
16	**2**	1 : 1 : 500	69	39 500	16 500	1.46

[a] Measured by the ^{1}H NMR spectroscopy. [b] Calculated M_n of PVL (g mol^{-1}): [δ-VL]:[cat]·conv·M(δ-VL) + M(BzOH); calculated Mn of PCL (g mol^{-1}): [ε-CL]:[cat]·conv·M(ε-CL) + M(BzOH). [c] Experimental M_n values were determined by SEC-MALS-VISCO analysis in THF solution.

biodegradable polyesters PLA, PVL and PCL. This mechanism opens the possibility of exchanging BzOH for polyalcohols, such as glycerol, trimethylolpropane, triethanolamine, pentaerythritol, xylitol, *myo*-inositol, D-sorbitol and dipentaerythritol as initiators. Therefore, **1** and **2** were tested in ROP of L-LA, δ-VL and ε-CL with these polyalcohols serving as the core in well-defined star-shaped polyesters (see Scheme 3).

The experimental set up was the same as in the case of the synthesis of linear polyesters. The polymerization reactions were carried out in a molar ratio of [catalyst] : [initiator] : [monomer] = 1 : 1/n : 100 (where n = number of hydroxyl groups in the initiator). The conversion of the polymerization experiments was monitored by the ^{1}H NMR spectroscopy. All isolated polymers were further characterized by the combined SEC-MALS-Visco analysis with the aim to determine the number-

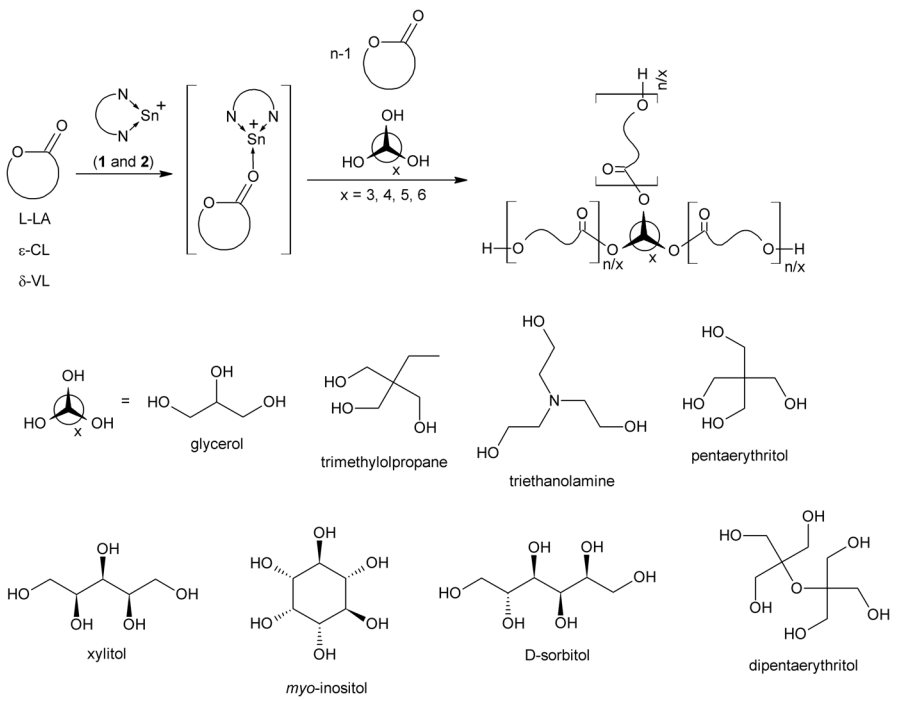

Scheme 3 Synthesis of star-shaped PLAs, PCLs and PVLs using **1** and **2** as catalysts.

Table 2 ROP of L-LA using catalysts **1** and **2** with a series of polyalcohols

Entry	Catalyst	Initiator	Conv[a] [%]	$M_{n,th}$[b] [g mol^{-1}]	$M_{n,SEC}$[c] [g mol^{-1}]	$Đ$	f[d]
1	**1**	Glycerol	96	13 900	6000	1.27	2.3 (3)
2	**1**	Trimethylolpropane	85	12 300	5700	1.16	2.5 (3)
3	**1**	Triethanolamine	96	13 900	6300	1.19	2.6 (3)
4	**1**	Pentaerythritol	96	13 900	9000	1.70	3.1 (4)
5	**1**	Xylitol	97	14 000	7700	1.91	3.7 (5)
6	**1**	*myo*-Inositol	88	12 700	10 100	1.51	2.7 (6)
7	**1**	D-Sorbitol	96	13 900	8200	1.80	4.1 (6)
8 (ref. 24)	**1**	Dipentaerythritol	95	13 950	8500	1.53	6.1 (6)
9	**2**	Glycerol	95	13 700	6800	1.09	2.6 (3)
10	**2**	Trimethylolpropane	89	12 800	9600	1.22	2.7 (3)
11	**2**	Triethanolamine	94	13 600	12 200	1.14	3.8 (3)
12	**2**	Pentaerythritol	97	14 000	11 900	1.45	3.6 (4)
13	**2**	Xylitol	97	14 000	13 200	1.32	4.4 (5)
14	**2**	*myo*-Inositol	85	12 300	8500	1.22	4.1 (6)
15	**2**	D-Sorbitol	94	13 600	12 700	1.57	5.2 (6)
16 (ref. 24)	**2**	Dipentaerythritol	96	14 100	13 200	1.15	7.2 (6)
17	**Sn(Oct)$_2$**	Dipentaerythritol	99	14 500	19 200	1.54	3.9 (6)

[a] Measured by the ^{1}H NMR spectroscopy. [b] Calculated M_n of PLA (g mol^{-1}): [L-LA]:[cat]·conv·M(L-LA) + M(initiator). [c] Experimental M_n values were determined by SEC-MALS-VISCO analysis in THF solution. [d] Numbers in parentheses indicate the theoretical number of arms.

average molar mass ($M_{n,SEC}$) and dispersity ($Đ$). These two macromolecular parameters further served as criteria for the classification of complexes **1** and **2** as suitable catalysts for well-controlled ROP. Thus, a promising catalyst should produce polymers with $Đ$ close to 1, indicating a uniform character of polymer. Furthermore, as already mentioned, $M_{n,SEC}$ should ideally be equal to the theoretical value of M_n ($M_{n,th}$) within well-controlled ROP. Results of the polymerization tests are summarized in Tables 2–4.

For L-LA, the polymerization tests did not show any significant effect of the used catalyst on the dispersity $Đ$, since it is statistical across the obtained PLAs (range of 1.09–1.91) but shows a relatively uniform nature of polymers. The lowest dispersity $Đ$ was achieved using catalytic system of **2** and glycerol (1.09, Table 2, entry 9). On the other, the complex **1** in the combination with xylitol produced polymer with the highest $Đ$ (1.91, Table 2, entry 5). A certain influence of the catalyst is evident in the case of number-average molar mass, when the experimental M_n values ($M_{n,SEC}$) for PLAs produced using catalyst **1** generally reach approximately half of the theoretical ones ($M_{n,th}$). On the other hand, when catalyst **2** is used, the agreement of these two parameters is observed, especially when triethanolamine, xylitol and D-sorbitol are used as initiators (Table 2, entries 11, 13 and 15). These results thus suggest better control by using of **2** as catalyst producing well defined uniform star-shaped polyesters of PLAs.

Table 3 ROP of δ-VL using catalysts **1** and **2** with a series of polyalcohol

Entry	Catalyst	Initiator	Conv[a] [%]	$M_{n,th}$[b] [g mol^{-1}]	$M_{n,SEC}$[c] [g mol^{-1}]	$Đ$	f[d]
1	**1**	Glycerol	93	9300	11 800	1.13	3.3 (3)
2	**1**	Trimethylolpropane	90	9000	9300	1.15	3.1 (3)
3	**1**	Triethanolamine	92	9200	9800	1.12	3.2 (3)
4	**1**	Pentaerythritol	97	9700	12 100	1.14	3.4 (4)
5	**1**	Xylitol	94	9400	9000	1.17	3.2 (5)
6	**1**	*myo*-Inositol	90	9000	3800	1.15	2.9 (6)
7	**1**	D-Sorbitol	91	9100	7600	1.17	3.4 (6)
8	**1**	Dipentaerythritol	92	9200	11 700	1.19	4.2 (6)
9	**2**	Glycerol	93	9300	14 600	1.96	7.3 (3)
10	**2**	Trimethylolpropane	90	9000	18 900	1.77	8.0 (3)
11	**2**	Triethanolamine	91	9100	14 900	1.87	7.2 (3)
12	**2**	Pentaerythritol	96	9600	19 000	1.72	7.8 (4)
13	**2**	Xylitol	95	9500	16 800	2.00	7.4 (5)
14	**2**	*myo*-Inositol	87	8700	14 400	1.89	8.4 (6)
15	**2**	D-Sorbitol	95	9500	15 800	2.13	8.1 (6)
16	**2**	Dipentaerythritol	90	9000	21 000	2.26	12 (6)
17	**Sn(Oct)$_2$**	Dipentaerythritol	93	9600	15 700	1.78	3.5 (6)

[a] Measured by the ^{1}H NMR spectroscopy. [b] Calculated M_n of PVL (g mol^{-1}): [δ-VL]:[cat]·conv·M(δ-VL) + M(initiator). [c] Experimental M_n values were determined by SEC-MALS-VISCO analysis in THF solution. [d] Numbers in parentheses indicate the theoretical number of arms.

Table 4 ROP of ε-CL using catalysts **1** and **2** with a series of polyalcohol

Entry	Catalyst	Initiator	Conv[a] [%]	$M_{n,th}$[b] [g mol^{-1}]	$M_{n,SEC}$[c] [g mol^{-1}]	$Đ$	f[d]
1	**1**	Glycerol	99	11 300	10 200	1.43	2.5 (3)
2	**1**	Trimethylolpropane	99	11 300	11 400	1.68	2.8 (3)
3	**1**	Triethanolamine	99	11 300	8800	1.34	2.4 (3)
4	**1**	Pentaerythritol	99	11 300	9500	1.73	2.7 (4)
5	**1**	Xylitol	99	11 300	8600	1.57	2.8 (5)
6	**1**	*myo*-Inositol	99	11 300	12 000	1.52	2.3 (6)
7	**1**	D-Sorbitol	99	11 300	10 000	1.70	3.2 (6)
8	**1**	Dipentaerythritol	99	11 300	6200	1.90	3.2 (6)
9	**2**	Glycerol	99	13 400	8300	1.63	7.1 (3)
10	**2**	Trimethylolpropane	65	13 000	10 200	1.38	4.5 (3)
11	**2**	Triethanolamine	95	13 100	8900	1.36	2.5 (3)
12	**2**	Pentaerythritol	99	13 900	9900	1.72	9.5 (4)
13	**2**	Xylitol	97	13 700	9700	3.18	14 (5)
14	**2**	*myo*-Inositol	67	12 600	12 000	1.53	2.3 (6)
15	**2**	D-Sorbitol	98	13 700	10 100	2.72	13 (6)
16	**2**	Dipentaerythritol	97	13 000	12 800	1.45	9.8 (6)
17	**Sn(Oct)$_2$**	Dipentaerythritol	99	11 500	16 400	1.68	3.7 (6)

[a] Measured by the ^{1}H NMR spectroscopy. [b] Calculated M_n of PCL (g mol^{-1}): [ε-CL]:[cat]·conv·M(ε-CL) + M(initiator). [c] Experimental M_n values were determined by SEC-MALS-VISCO analysis in THF solution. [d] Numbers in parentheses indicate the theoretical number of arms.

In contrast, the polymerization experiments of δ-VL indicated strong influence of catalyst on dispersity $Đ$ of isolated star-shaped PVLs. It is evident, that complex **1** produce polymers with very low dispersity $Đ$, which is in a very narrow range of 1.12–1.19 (Table 3, entries 1–8). Moreover, $M_{n,SEC}$ values correlate very well with $M_{n,th}$, except for the case involving *myo*-inositol (Table 3, entry 6). In contrast, poor control over polymerization was achieved when complex **2** was used as catalyst. The isolated star-shaped PVLs revealed dispersity $Đ$ of range 1.72–2.26 (Table 3, entries 9–16) and $M_{n,SEC}$ values are almost twice as large as $M_{n,th}$. These results thus suggest better control by using of **1** as catalyst producing well defined uniform star-shaped of PVLs.

Similar results were also obtained in the polymerization experiments of ε-CL. In comparison to the ROP of L-LA and δ-VL, the polymerization of ε-CL is less controlled, but complex **1** produce star-shaped polyesters with narrower dispersity $Đ$ ranging from 1.34 to 1.90 (Table 4, entries 1–8) and $M_{n,SEC}$ values correlate with $M_{n,th}$, except for the dipentaerythritol (Table 4, entry 8). Poor control over polymerization was achieved when complex **2** was used as catalyst (dispersity $Đ$ ranging from 1.36 to 3.18, Table 4, entries 9–16). These results thus again suggest better control by using of **1** as catalyst producing well defined uniform star-shaped polyesters of PCLs.

The different ability of complexes **1** and **2** to control the polymerization of L-LA, δ-VL and ε-CL, and thus the dispersity $Đ$, can be explained based on the strength of the interaction between the catalyst (as Lewis acid) and the monomer (as Lewis base) in the activated monomer. This is a prerequisite to produce well-defined polymers. In the previous work, we used theoretical calculations to determine the NPA atomic charge q of tin(II) atom in **1** and **2**, which are 1.42e (for **1**) and 1.21 (for **2**) indicating **1** as more Lewis acidic.[24] Unfortunately, to the best of our knowledge, there is no study in the literature comparing the basicity of L-LA, d-VL and e-CL. Information about this is only for δ-VL and ε-CL, which exhibit similar pK_b (14.3 for δ-VL and 14.7 for ε-CL).[27] However, it can be assumed that the presence of a Me group with a +I effect in the L-LA structure increases the nucleophilic character of the carbonyl oxygen, and thus the Lewis basicity. The Lewis basicity of the studied monomers can thus be estimated in order L-LA > δ-VL ≈ ε-CL. From this point of view, δ-VL and ε-CL can form a strong interaction only with more Lewis acidic complex **1**, leading to well-defined star-shaped PVLs and PCLs. In contrast, L-LA can also interact strongly with complex **2**, which, despite the assumption of a weaker interaction than in the case of complex **1**, produces PLAs with a lower distribution.

The incorporation of polyalcohols into the polymer chain was confirmed by ^{1}H NMR spectroscopy. A representative sample was chosen for this study, namely PCL containing trimethylolpropane as the core (Table 4, entry 2). In the ^{1}H NMR spectrum of this polymer, the major signals with $\delta = 1.28$, 1.55, 2.21 and 3.96 ppm corresponding to CH_2 protons of the main chain of ε-caprolactone unit were found. Besides these signals, the ^{1}H NMR spectrum revealed small peaks with $\delta = 0.80$ and 3.89 ppm, which were assigned to the trimetholpropane core. In addition, the presence of trimethylolpropane in the prepared PCL was also detected by TG-GCMS, when the chromatogram of the studied PCL showed a peak with a retention time of t_R = 3.6 min and $M_w = 134$.

Although these studies confirm the incorporation of polyalcohols into the structure of the prepared polymers, the branching of the polymer chain cannot be clearly determined from these data. The combined SEC-MALS-viscosity method allows not only the determination of absolute molar mass distribution, but also the estimation of the degree of branching. The detection and quantification of branching is based on the fact that a branched macromolecule has smaller size than corresponding linear molecule of identical chemical composition and molar mass.[28] For small macromolecules the branching

cannot be characterized on the basis of root mean square radius (radius of gyration) as this quantity cannot be determined for molecules with radii below about 10 nm, which roughly corresponds to molar mass of 10^5 g mol^{-1}. This limit applies to majority of molecules in the prepared samples. Instead, branching characterization based on the intrinsic viscosity can be used:[29]

$$g' = \left(\frac{[\eta]_{br}}{[\eta]_{lin}}\right)_M \quad (1)$$

Here $[\eta]$ is the intrinsic viscosity of branched (br) and linear (lin) macromolecule, subscript M refers to the same molar mass. The parameter g' can be related with the number of arms. The equation derived by Douglas *et al.*[30a] was used in this work:

$$g' = \left(\frac{3f-2}{f^2}\right)^{0.58} \frac{0.724 - 0.015(f-1)}{0.724} \quad (2)$$

Here f is the number of arms per branched macromolecule. To obtain the branching ratio g', one needs constants of Mark–Houwink equation for linear polymer. The constants were obtained by plotting the Mark–Houwink plots obtained by the SEC-MALS-viscosity analysis of linear PLA, PCL and PVL samples. To cover the molar mass range as broad as possible, Mark–Houwink plots of four different samples of different molar mass distribution were gathered together. The plots of linear polymers obtained by ROP catalysed by **2** (PLA) and **1** (PVL and PCL) that showed better control over the polymerization are depicted in Fig. 1 and the Mark–Houwink constants obtained from these plots are as follows:

$$\text{PLA } [\eta] = 0.025 \times \text{M}^{0.755}$$

$$\text{PCL } [\eta] = 0.042 \times \text{M}^{0.692}$$

$$\text{PVL } [\eta] = 0.051 \times \text{M}^{0.659}$$

The constants are valid for THF and 25 °C. Using the above equations, one can calculate the intrinsic viscosity of a hypothetical linear polymer that would have the same weight-average molar mass (M_w) as that of branched polymer (see Fig. 2). The branching ratio g' is obtained by simple division of the experimental weight-average intrinsic viscosity ($[\eta]_w$) divided by the value calculated for the linear polymer (see Fig. 2). The estimation of an average number of arms per molecules is performed using the eqn (2). As eqn (2) does not allow the explicit expression for f, one can simply calculate g' for various f (with an increment 0.1) in Excel, and then to match the g' calculated for a given sample with f. The obtained values of f are listed in Tables 2–4.

In the case of star-shaped PLAs, the factor f ranges from 2.3 to 5.2 and thus the experimental number of arms is always slightly lower than the theoretical ones. As discussed, complex **2** showed better control over the polymerization of the star shaped polymers. This is also demonstrated by the values of the factor f ranging from 2.6 to 5.2. Therefore, the values correlate well with the theoretical ones, except the star shaped polymer based on *myo*-inositol as a core (Table 2, entry 14). As already mentioned, polymerization tests of δ-VL producing star-shaped PVLs showed better control when using catalyst **1**. This fact is

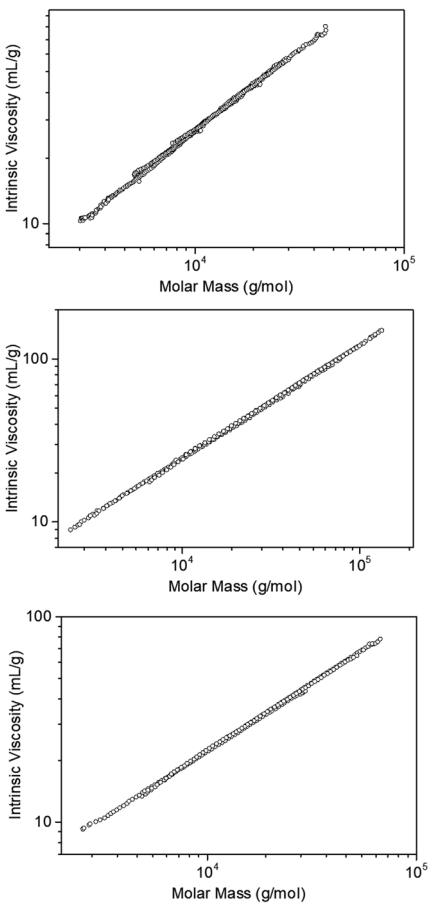

Fig. 1 Mark–Houwink plots of linear PLA (top), PCL (center), and PVL (bottom).

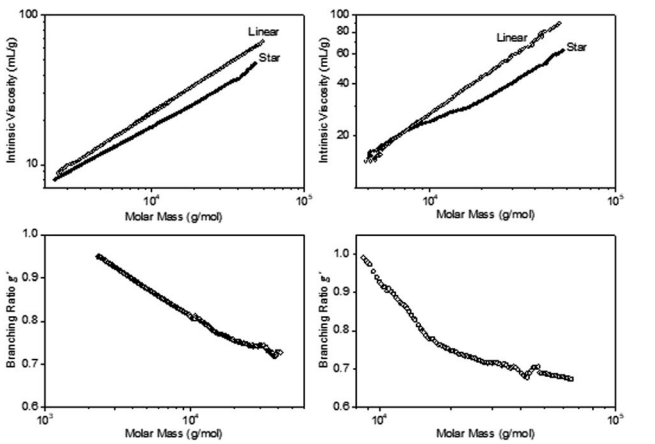

Fig. 2 Example of Mark–Houwink plots of linear and star shaped polymers. Top left: PVL, linear *vs.* star shaped with theoretically four arms (pentaerythritol as core, Table 3, entry 4) catalysed by 1; left bottom: g'–versus–M plot for the star shaped PVL; top right: PLA, linear *vs.* star shaped with theoretically four arms (pentaerythritol as core, Table 2, entry 12) catalysed by 2; left bottom: g'–versus–M plot for the star shaped PLA.

also reflected in factor f ranging from 2.9 to 4.2. The values thus fit well especially in the case of 3- and 4-armed star-shaped PVLs (Table 3, entries 1–4), while 5- and 6-armed PVLs revealed lower branching. The biggest discrepancy can be found again for *myo*-inositol as a core (Table 3, entry 6). Similar results can be found for star-shaped PCLs, where better control was achieved by catalyst **1**. The factor f ranges from 2.3 to 3.2. The values again fit well for 3- and 4-armed star-shaped PCLs (Table 4, entries 1–4), while 5- and 6-armed PCLs revealed lower branching. The biggest discrepancy can be found again for *myo*-inositol as a core (Table 4, entry 6).

Finally, the catalytic activity of complexes **1** and **2** was compared with commercial $Sn(Oct)_2$. Dipentaerythritol was selected as representative initiator. The experimental set up was the same as in the case of complexes **1** and **2**. The macromolecular parameters $M_{n,SEC}$, $Đ$ and f are summarized in Tables 2–4 (for PLA, see Table 2 entry 17; for PVL, see Table 3, entry 17 and for PCL, see Table 4, entry 17). For all polymers $M_{n,SEC}$ is higher than $M_{n,th}$, the deviation is more pronounced than for their analogues prepared using **2** (for PLA and PCL) and **1** (for PVL). The dispersity $Đ$ is also higher (1.54 *vs.* 1.15 for PLA, 1.78 *vs.* 1.19 for PVL and 1.68 *vs.* 1.45). Additionally, $Sn(Oct)_2$ does not provide polymers with such a degree of branching compared to **2** and **1** (3.9 *vs.* 7.2 for PLA, 3.5 *vs.* 4.2 for PVL and 3.7 *vs.* 9.8 for PCL). By comparing these factors, it can be clearly stated that complex **2** (for PLA and PCL) and complex **1** (for PVL) control ROP much more effectively than commercial $Sn(Oct)_2$.

Comparison of wettability of linear and star-shaped polyesters

As it has been stated linear PLA and PCL based materials are considered as hydrophobic materials.[3] Thus, the comparison of the wettability of linear and star-shaped PLA, PCL and PVL prepared in this study was another goal. Since the literature clearly demonstrates dependence of the WCAs on the fabrication method, we took advantage of the good solubility of the synthesized polymers and we prepared thin layers of above mentioned polymers by an spin-coating method to avoid any influence on the method of fabrication. This method may provide thin layers with uniform surfaces and allow us to study the hydrophobicity of the polymers in terms of composition, structure, and concentration.

To investigate the influence of WCA on the polymer composition, linear polyesters with similar M_n prepared by ROP catalysed by **1** or **2** were selected. Thus the linear PLA (**PLA-L**) with $M_n = 7800$ g mol^{-1} and $Đ = 1.25$,[24] linear PVL (**PVL-L**) with $M_n = 7200$ g mol^{-1} and $Đ = 1.53$ (see Table 1, entry 6) and linear PCL (**PCL-L**) with $M_n = 8000$ g mol^{-1}, $Đ = 1.55$ (see Table 1, entry 10) were studied further. To see the effect of the polymer structure on WCA, star-shaped polyesters with similar M_n derived from dipentaerythritol as polymers with the highest number of arms prepared by ROP catalysed by **1** or **2** were selected. Thus the star-shaped PLA (**PLA-DPE**) with M_n = 13 200 g mol^{-1}, $Đ = 1.15$ and $f = 7.2$ (see Table 2, entry 16),[24] star-shaped PVL (**PVL-DPE**) with $M_n = 11\,700$ g mol^{-1}, $Đ = 1.19$ and f = 4.2 (see Table 3, entry 8) and star-shaped PCL (**PCL-DPE**) with M_n = 12 800 g mol^{-1}, $Đ$ = 1.45 and f = 9.8 (Table 4, entry 16) were studied further. We tested THF solutions of selected polymers at concentrations 0.5, 1.0 and 2.0% (w/w) for the fabrication of the thin layers. A silicon wafer was used as a substrate to may analysed these thin layers based on atomic force microscopy (AFM), scanning electron microscopy (SEM) and variable angle spectroscopic ellipsometry (VASE) data. The thin layers were fabricated by the coating on the silicon wafer with approximately 0.3 ml of the THF solutions of polymers followed by the spinning at 4000 rpm. Then, the thin layers were dried under vacuum. The substrates modified in this way were subsequently used for the measurement of WCA by the sessile drop method. The obtained results of these measurements are summarized in Fig. 3 and Table S1 in ESI.†

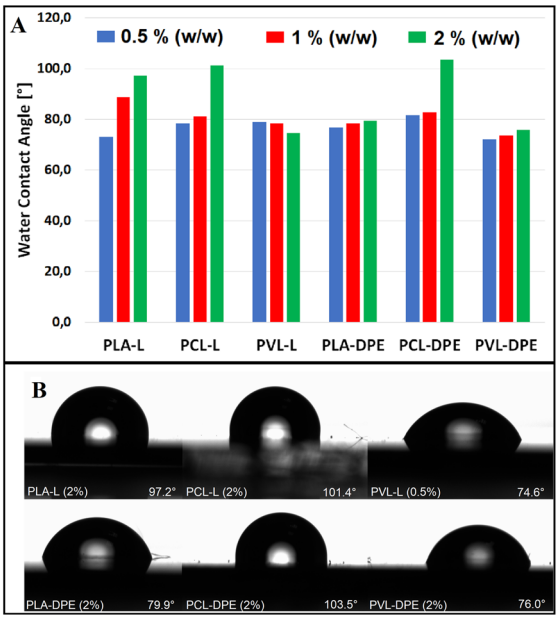

Fig. 3 (A) A graphical representation of WCAs of tested linear and star-shaped polymers. (B) Screens of water droplet.

The measured data show that WCA depends on polymer composition, polymer structure and concentration. In general, the most hydrophobic materials were obtained from 2% (w/w) solutions. The highest WCA values were found for 2% (w/w) **PLA-L** (97.2°), 2% (w/w) **PCL-L** (101.4°) and 2% (w/w) **PCL-DPE** (103.5°) and fall in the region of hydrophobic behaviour. Therefore, the influence of the polymer composition on WCA is evident, since hydrophobic properties are mainly exhibited by both PCLs, while both polymers based on PVLs are hydrophilic (**PVL-L** 74.6°, **PVL-DPE** 76.0°). The influence of the polymer structure on WCA can be also discussed. While the WCAs of polymers based on PVL and PCL are almost the same for both linear and star-shaped analogues, pronounced effect is observed for PLA polymers. The star-shaped **PLA-DPE** (2% (w/w)) has a hydrophilic character with WCA not exceeding 79.9°, while linear **PLA-L** (2% (w/w)) revealed hydrophobic behaviour with WCA at 97.2°. These results again proved that the values of WCA of polymer materials strongly depend on the method of the preparation and the WCA of spin-coated thin layers of PLA, PCL or PVL cannot compete with PLA nanofibers prepared by

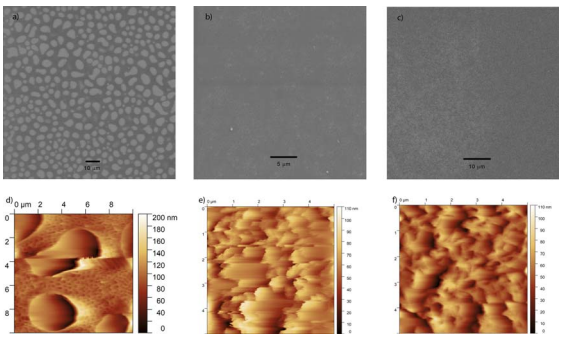

Fig. 4 SEM image and AFM scan of **PLA-L** (a, d), **PCL-L** (b, e) and **PCL-DPE** (c, f).

Table 5 Characteristics of prepared thin layers: thickness films (determined by VASE) – error in determination of thickness is ±2 nm, RMS (determined by AFM) – error in determination of thickness is ±2 nm

Thin layer			
Sample name	WCA [°]	Thickness [nm]	RMS [nm]
2% (w/w) **PLA-L**	97 (±1)	155	20.36
2% (w/w) **PCL-L**	101 (±1)	222	16.59
0.5% (w/w) **PVL-L**	75 (±2)	52	Macro defects
2% (w/w) **PLA-DPE**	80 (±1)	154	Macro defects
2% (w/w) **PCL-DPE**	104 (±3)	242	14.42
2% (w/w) **PVL-DPE**	76 (±3)	44	6.31

the electrospinning method, where WCA exceeding 150° were obtained.[3m]

As mentioned, the uniformity of thin layers was also studied. Surfaces were characterized based on atomic force microscopy (AFM), scanning electron microscopy (SEM) and variable angle spectroscopic ellipsometry (VASE) data. The SEM and AFM data showed that thin layers of hydrophobic materials have the surface with small cracks and corrugations (Fig. 4) with root mean square (RMS) roughness values (determined by AFM) in the narrow range of 14.42–20.36 nm. The thicknesses of these thin layers (determined by VASE) showed also narrow values of 155–242 nm (Table 5).

In contrast, the VASE data revealed that thin layers of hydrophilic materials have smaller thicknesses ranging from 44

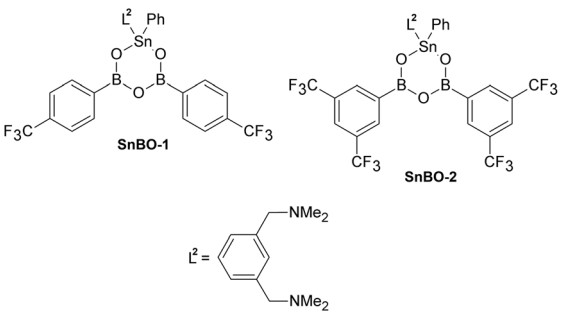

Fig. 5 Structure of stannaboroxines **SnBO-1** and **SnBO-2**.

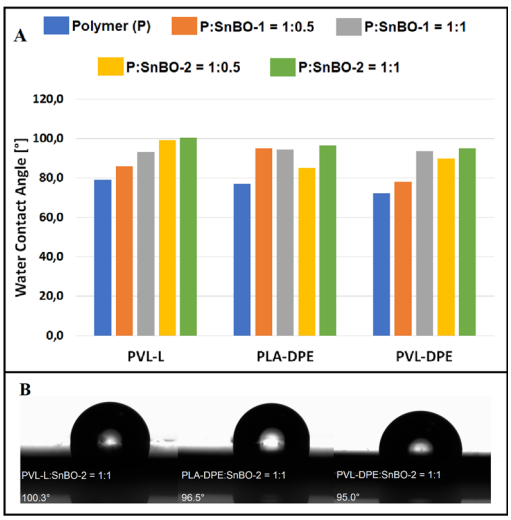

Fig. 6 (A) A graphical representation of the WCA of tested formulations containing **SnBO-1** and **SnBO-2**. (B) Screens of water droplet.

to 154 nm (Table 5), and the SEM and AFM data suggested that the surfaces of two samples contain macro defects and therefore AFM scans could not be measured (see Table 5).

To increase the hydrophobic properties of the studied polymers, we further focused our attention on their combination with another component. In the past decade, we have been concerned with the synthesis of N → M coordinated galla- or stannaboroxines with the general formula $L^2Ga(OB\text{-}Ar)_2O$ and $L^2(Ph)Sn(OB\text{-}Ar)_2O$ containing MB_2O_3 central ring ($L^2 = C_6H_3\text{-}2,6\text{-}(Me_2NCH_2)_2$, Ar = substituted aryl).[25] The great advantage of this type of compounds is easy preparation, solubility in organic solvents and great variability of differently substituted aryls bound to the boron atoms. In addition, it has recently been found that gallaboroxine $LGa(OB\text{-}Ar)_2O$, where Ar is C_6H_4-4-CH = O, exhibits very good film-forming properties, which allowed the fabrication of transparent thin films with properties comparable to amorphous oxide glasses containing B_2O_3 and Ga_2O_3 (ref. 31) (for example refractive index $n = 1.44$ or optical band gap $E_g = 3.95$ eV).[25a] This fact evoked us to use heteroboroxines as additives to the studied polymers to improve the

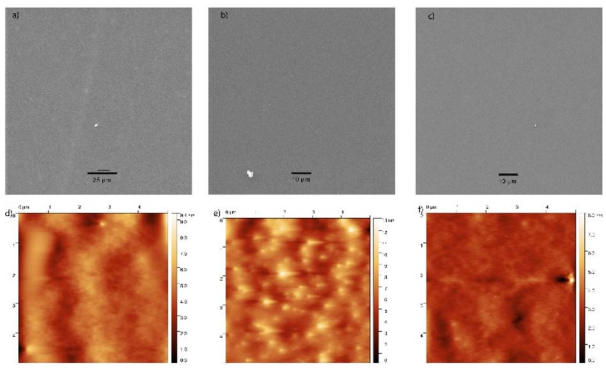

Fig. 7 SEM image and AFM scan of **PVL-L** : **SnBO-2** = 1 : 1 (w/w) (a, c), **PLA-DPE** : **SnBO-2** = 1 : 1 (w/w) (b, e) and **PVL-DPE** : **SnBO-2** = 1 : 1 (w/w) (c, f).

Table 6 Characteristics of prepared thin layers: thickness films (determined by VASE) – error in determination of thickness is ±2 nm, RMS (determined by AFM) – error in determination of thickness is ±0.2 nm for **SnBO-2** based thin layers

Thin layer				
Sample name	WCA [°]	The increase of WCA [°]	Thickness [nm]	RMS [nm]
0.5% (w/w) **PVL-L : SnBO-2** 1 : 1	100 (±1)	25.7	465	0.94
2% (w/w) **PLA-DPE : SnBO-2** 1 : 1	97 (±2)	15.7	522	1.18
2% (w/w) **PVL-DPE : SnBO-2** 1 : 1	95.0 (±1)	19	89	0.66

uniformity of surfaces and increase the WCAs of these hydrophilic materials. Two stannaboroxines $L^2(Ph)Sn[(OB\text{-}(C_6H_4\text{-}4\text{-}CF_3))_2O]$ (**SnBO-1**) and $L^2(Ph)Sn[(OB\text{-}(C_6H_4\text{-}3,5\text{-}CF_3)_2)_2O]$ (**SnBO-2**) (Fig. 5),[25b] were selected due to their solubility. The presence of fluorine atoms in the structures of **SnBO-1** and **SnBO-2** could have been a promising aspect to increase the WCA. In addition, both compounds contain six-membered SnB_2O_3 central core and they structurally resemble polymer N-Boroxine-PDMS with six-membered B_3O_3 central core.[26]

Therefore, THF solutions of **PVL-L** (0.5% w/w), **PLA-DPE** (2% w/w), and **PVL-DPE** (2% w/w) were enriched by **SnBO-1** and **SnBO-2** to get two ratios of polymer/SnBO at 1 : 0.5 and 1 : 1, respectively. Thus, new formulations were obtained for the study of hydrophobic properties.

The thin layers from these THF solutions of new SnBO based formulations were fabricated by similar way (spin coating on the silicon wafer) and dried under vacuum. The substrates modified in this way were subsequently used for the measurement of WCA by the sessile drop method. The obtained results of these measurements are summarized in Fig. 6 and Table S2 in ESI.†

Based on these data, it was found that the addition **of SnBO-2** with the ratio of polymer/**SnBO-2** at 1 : 1 significantly increased the WCAs of thin layers of **PVL-L**, **PLA-DPE** and **PVL-DPE**. Their hydrophilic character was changed to the hydrophobic one with the WCAs 100.3° (**PVL-L**), 96.5° (**PLA-DPE**) and 95.0° (**PVL-DPE**). Especially for **PVL-L**, the increase of WCA (25.7°) is the most striking. Of course, **SnBO-1** and **SnBO-2** were also added to **PLA-L**, **PCL-L** and **PCL-DPE** and new formulations were fabricated in the same way. However, such a significant improvement in hydrophobic properties was not observed in these cases (Table S2 and Fig. S1, ESI†).

The uniformity of these thin layers with highest WCAs (Polymer : **SnBO-2** = 1 : 1 (w/w)) was again studied. Surfaces were characterized based on AFM, SEM and VASE. The SEM and AFM data showed smooth surface without cracks and corrugations (see Fig. 7). Root mean square (RMS) roughness values determined by AFM were typically found to be lower than ∼2.35 nm (see Table 6). The thicknesses of all samples were determined by VASE showing values of 89–522 nm (Table 6). From these data, it is evident that the hydrophobicity is not influenced by the thickness of layers, which varies between 89 and 522 nm with almost the same WCAs (95–100°). In addition, the presence of oxygen, boron, fluorine and tin atoms in the spin coated thin films was confirmed by SEM EDX.

Therefore, it is evident, that the stannaboroxines improved the uniformity of surfaces of thin layers of polymers and increased the WCAs of these hydrophilic materials and formed the hydrophobic materials.

Conclusions

Following the catalytic activity of N-coordinated tin(II) cations $[L^1 \rightarrow Sn(H_2O)][OTf]_2 \cdot THF$ (**1**) and $[L^1 \rightarrow SnCl][SnCl_3]$ (**2**) in ROP producing well-defined linear PLAs *via* activated monomer mechanism, here, we determined these complexes as effective and universal also for the polymerization of ε-CL and δ-VL. The polymerization of these monomers yielded well-defined linear PCL and PVL. Moreover, the formation of activated monomer opened the possibility to use different polyalcohols for the synthesis of well-defined star-shaped analogues. Thus, the application of **1** and **2** in the synthesis of star-shaped polyesters PLAs, PVLs and PCLs led to the preparation of a series of polymers with different arm numbers. While well-defined star-shaped PLAs were obtained using complex **2**, complex **1** provided well-defined star-shaped PVLs and PCLs.

The preparation of well-defined linear and star-shaped PLAs, PCLs and PVLs allowed us to compare their wettability in terms of composition and polymer structure. For this study, thin layers of the linear and six-armed polymers derived from dipentaerythritol were fabricated by spin-coating method to avoid any influence on the method of fabrication. Results based on WCA measurements showed that the wetting properties of PCLs and PVLs depend only on the composition, when PCLs showed hydrophobic character (∼102°), while PVLs hydrophilic (∼75°). For PLAs, the hydrophobicity was found for linear polymer (∼97°), while star-shaped analogue (∼80°) showed the hydrophilicity. To improve the uniformity of surfaces and increase the WCAs, two stannaboroxines $L^2(Ph)Sn[(OB\text{-}(C_6H_4\text{-}4\text{-}CF_3))_2O]$ and $L^2(Ph)Sn[(OB\text{-}(C_6H_4\text{-}3,5\text{-}CF_3)_2)_2O]$ were applied. The addition of stannaboroxines improved the uniformity of thin films and moreover transferred hydrophilic polyesters to hydrophobic, which was the most striking for linear PVL (ΔWCA ∼26°). This fact suggested the use of stannaboroxines and other heteroboroxines can be promising approach for the creating of hydrophobic materials.

Experimental part

General consideration

All moisture and air sensitive reactions were carried out under an argon atmosphere using standard Schlenk tube techniques.

All solvents were dried using Pure Solv–Innovative Technology equipment. L-lactide, δ-valerolactone and ε-caprolactone were purchased from Sigma-Aldrich and were purified by the recrystallization from toluene or distillation over CaH_2 before use. Compounds **1**, **2**, **SnBO-1** and **SnBO-2** were prepared according to the literature.[24,25b] The ^{1}H NMR spectra were recorded on a Bruker 500 NMR spectrometer at 298 K. The ^{1}H NMR spectra were referenced internally to the residual protio-solvent. The molar mass distributions and Mark–Houwink plots were determined by size exclusion chromatography (SEC) coupled with a multi-angle light scattering (MALS) detector DAWN NEON, an RI detector Optilab NEON and an online viscometer ViscoStar NEON (all detectors from Wyatt Technology). The SEC system consisted of a 1200 Series isocratic pump and an autosampler with two Mixed-C 300 × 7.5 mm 5 μm columns (all Agilent Technologies) using tetrahydrofuran (THF) as the mobile phase at a flow rate of 1 ml min^{-1}. Samples of linear and star-branched polymers were prepared as solutions in THF at the concentrations of ≈ 6 mg ml^{-1}, left to dissolve for at least 12 h, filtered with 0.45 μm filters and injected in the amount of 100 μL. The specific refractive index increment (dn/dc) was determined from the RI detector response and injected mass assuming 100% mass recovery. The average values obtained from four or five measurements of different linear samples are as follows:

$$\text{PLA } dn/dc = 0.046 \pm 0.001 \text{ ml g}^{-1}$$

$$\text{PCL } dn/dc = 0.072 \pm 0.001 \text{ ml g}^{-1}$$

$$\text{PVL } dn/dc = 0.070 \pm 0.001 \text{ ml g}^{-1}$$

The values are valid for THF, the wavelength 690 nm and temperature 25 °C.

Ring-opening polymerization of L-lactide using 1 and 2 as catalysts. Typical polymerization procedures are as follows. A catalyst, benzylalcohol or polyalcohol and monomer in a molar ratio 1 : 1/n : 100 (where n = number of hydroxyl groups in the initiator) were weighted into a Schlenk tube and homogenized. The polymerization mixture was then placed into an oven pre-heated to 145 °C. After a desired time, the reaction mixture was cooled to room temperature and subjected to the ^{1}H NMR analysis. The monomer conversion was determined by the calculation of the integration of the monomer *vs.* polymer characteristic resonances in the ^{1}H NMR ($CDCl_3$, 500 MHz) spectrum. The polymer was purified by dissolving the crude samples in $CHCl_3$ and precipitating into cold methanol (100 ml). The obtained polymers were dried to a constant weight, and the dry polymer samples were analyzed by the SEC-MALS-Visco.

Preparation of thin layers of linear and star-shaped polymers by spin-coating. The polymer samples were dissolved in THF at concentrations of 0.5, 1 and 2% (w/w). For example, for 2% (w/w) solution: 0.2 g of polymer was dissolved in 9.80 g of THF.

The prepared solutions were deposited on silicon wafer substrates of 15 × 15 × 0.3 mm and the substrates were rotated using a Spin-Master spin coater at 4000 rpm for 60 s. After that, thin layers were dried under vacuum at 80 °C. The formulations containing the stannaboroxines **SnBO-1** and **SnBO-2** were prepared by adding these compounds to appropriate THF polymer solution in weight ratios of polymer:**SnBO-1(-2)** at 1 : 0.5 and 1 : 1. For example, for formulation of 2% (w/w) solution of polymer with **SnBO-2** in ratio 1 : 1 (w/w): 0.2 g of polymer and 0.2 g of **SnBO-2** was dissolved in 9.80 g of THF. The thin films were prepared in the same manner as the polymer samples themselves.

Water contact angles (WCAs) measurements. The WCAs by the sessile drop method were measured using an OCA 50EC goniometer (DataPhysics Instruments). Data were collected with OCA20 software. The volume of dispensed water was set to 3.5 μl. 10 images were taken from one drop and the determinations were made on 3 different locations for each condition. The resulting WCAs were averaged.

Characterization of thin layers prepared by spin-coating. The surface of the prepared films and their chemical composition were studied using scanning electron microscopy (SEM, TESCAN, VEGA 3, EasyProbe, Brno, Czech Republic) linked with energy-dispersive X-ray analyzer. The EDX measurements were performed at 3 spots per sample. Atomic force microscopy (Solver NEXT, NT-MDT) was used to study topography of thin films within typical scanned area of 5 μm × 5 μm and 10 μm × 10 μm. Measured data were edited by means of rows alignment using polynomial function of the fourth order. The AFM scans were performed in the semi-contact mode (amplitude modulated atomic force microscopy – AM-AFM) using double-sided cantilever with the resonant frequency of 235 and 140 kHz (±10%) respectively. The data were proceeded using Gwyddion software. Optical functions of prepared layers as well as their thicknesses were obtained from the analysis of spectroscopic ellipsometry data measured using an ellipsometer with automatic rotating analyzer (VASE, J. A. Woollam Co., Inc.). Experimental data were analyzed using a three layer model of optical functions: (i) the substrate (silicon substates), (ii) thin film, and (iii) the surface layer. For the analysis of VASE data in broad measured spectral region (300 nm–2300 nm, with wavelengths steps of 20 nm and angles of incidence 65°, 70° and 75°.), we used Cauchy model.

Data availability

All data generated or analyzed during this study are included in this published article and its ESI files.† For more details, please contact authors.

Conflicts of interest

There are no conflicts to declare.

Acknowledgements

The authors would like to thank the Czech Science Foundation (no. 23-06548S) for the financial support.

Notes and references

1 (*a*) E. Chiellini and R. Solaro, *Adv. Mater.*, 1996, **8**, 305; (*b*) S. Mecking, *Angew. Chem., Int. Ed.*, 2004, **43**, 1078; (*c*) L. S. Nair and C. T. Laurencin, *Prog. Polym. Sci.*, 2007, **32**, 762–798; (*d*) B. Laycock, M. Nikolić, J. M. Colwell, E. Gauthier, P. Halley, S. Bottle and G. George, *Prog. Polym. Sci.*, 2017, **71**, 144; (*e*) R. H. Platel, L. M. Hodgson and C. K. Williams, *Polym. Rev.*, 2008, **48**, 11; (*f*) G. Barouti, K. Jarnouen, S. Cammas-Marion, P. Loyer and S. M. Gaillaume, *Polym. Chem.*, 2015, **6**, 5414; (*g*) X. Zhang, M. Fevre, G. O. Jones and R. M. Waymouth, *Chem. Rev.*, 2018, **18**, 839; (*h*) M. Suzuki, Y. Tachibana, K. Oba, R. Takizawa and K.-I. Kasuya, *Polym. Degrad. Stab.*, 2018, **149**, 1.

2 (*a*) L. Fambri and C. Migiliaresi, Crystallization and thermal properties, in *Poly(lactic Acid): Synthesis, Structures, Properties, Processing and Applications*, ed. R. Auras, L. T. Lim, S. E. M. Selke and H. Tsuji, John Wiley & Sons Inc, New York, 2010, pp. 113–124; (*b*) M. K. Nampoothiri, N. R. Nair and R. P. John, *Bioresour. Technol.*, 2010, **101**, 8493; (*c*) M. Jamshidian, E. A. Tehrany, M. Imran, M. Jacquot and S. Desobry, *Compr. Rev. Food Sci. Food Saf.*, 2010, **9**, 552; (*d*) A. Jahandideh and K. Muthukumarappan, *Eur. Polym. J.*, 2017, **87**, 360; (*e*) E. S. Kim, B. C. Kim and S. H. Kim, *J. Polym. Sci., Part B: Polym. Phys.*, 2004, **42**, 939; (*f*) M. B. Khajeheian and A. Rosling, *J. Appl. Polym. Sci.*, 2016, **13**, 42231/1–8.

3 (*a*) A. Cipitria, A. Skelton, T. R. Dargaville, P. D. Dalton and D. W. Hutmacher, *J. Mater. Chem.*, 2011, **21**, 9419; (*b*) A. Martins, E. D. Pinho, S. Faria, I. Pashkuleva, A. P. Marques, R. L. Reis and N. M. Neves, *Small*, 2009, **5**, 1195; (*c*) F. Yang, J. G. C. Wolke and J. A. Jansen, *Chem. Eng. J.*, 2008, **137**, 154; (*d*) E. V. Melnik, S. N. Shkarina, S. I. Ivlev, V. Weinhardt, T. Baumbach, M. V. Chaikina, M. A. Surmeneva and R. A. Surmenev, *Polym. Degrad. Stab.*, 2019, **167**, 21; (*e*) Š. Zupančič, L. Preem, J. Kristl, M. Putrinš, T. Tenson, P. Kocbek and K. Kogermann, *Eur. J. Pharm. Sci.*, 2018, **122**, 347; (*f*) H. Jeon and G. Kim, *J. Mater. Chem. B*, 2014, **2**, 171; (*g*) S. Surucu, K. Masur, H. Turkoglu Sasmazel, T. Von Woedtke and K. D. Weltmann, *Appl. Surf. Sci.*, 2016, **385**, 400; (*h*) N. E. Zander, J. A. Orlicki, A. M. Rawlett and T. P. Beebe, *ACS Appl. Mater. Interfaces*, 2012, **4**, 2074; (*i*) J. Shi, N. M. Alves and J. F. Mano, *Bioinspiration Biomimetics*, 2008, **3**, 034003; (*j*) E. H. Tümer, H. Y. Erbil and N. Akdogan, *Langmuir*, 2022, **38**, 10052; (*k*) X.-Q. Cheng, W. Liu, Ch. Zhang, X.-Ch. Chen, S.-Q. Duan and H. Fu, *J. Appl. Polym. Sci.*, 2022, **139**, e52621; (*l*) J. Kingman and M. K. Dymond, *Chem. Data Collect.*, 2022, **40**, 100884; (*m*) P. M. Gorea and B. Kandasubramanian, *J. Mater. Chem. A*, 2018, **6**, 7457; (*n*) D. Zhang, X.-Z. Jin, T. Huang, N. Zhang, X.-D. Qi, J.-H. Yang, Z.-W. Zhou and Y. Wang, *ACS Appl. Mater. Interfaces*, 2019, **11**, 5073; (*o*) Ch. Eang and P. Opaprakasit, *J. Polym. Environ.*, 2020, **28**, 1484; (*p*) W. Li, Q. Yu, H. Yao, Y. Zhu, P. D. Topham, K. Yue, L. Ren and L. Wang, *Acta Biomater.*, 2019, **92**, 60; (*q*) F. Wang, K. Liu, Y. Xi and Z. Li, *Polymer*, 2022, **249**, 124858; (*r*) G. Zhang, P. Wang, X. Zhang, Ch. Xiang and L. Li, *Eur. Polym. J.*, 2019, **116**, 386.

4 (*a*) W. Zhang, T. Ji, S. Lyon, M. Mehta, Y. Zheng, X. Deng, A. Liu, A. Shagan, B. Mizrahi and D. S. Kohane, *ACS Appl. Mater. Interfaces*, 2020, **12**, 17314; (*b*) Y. Deng, S. J. Liu, B. M. Zhao, P. Wang, Q. L. Fan, W. Huang and L. H. Wang, *J. Lumin.*, 2011, **131**, 2166; (*c*) L. Teng, X. Xu, W. Nie, Y. Zhou, L. Song and P. Chen, *J. Polym. Res.*, 2015, **22**, 83; (*d*) I. Yu, T. Ebrahimi, S. G. Hatzikiriakos and P. Mehrkhodavandi, *Dalton Trans.*, 2015, **44**, 14248; (*e*) B. S. Lele and J. C. Leroux, *Polymer*, 2002, **43**, 5595.

5 S. H. Luo, Q. F. Wang, J. F. Xiong and Z. Y. Wang, *J. Polym. Res.*, 2019, **19**, 9962/1–9.

6 (*a*) S. H. Kim and Y. H. Kim, *Macromol. Symp.*, 1999, **144**, 277; (*b*) H. Tsuji and M. Suzuki, *Macromol. Chem. Phys.*, 2014, **215**, 1879; (*c*) Y. Lin, A. Zhang and L. Wang, *J. Appl. Polym. Sci.*, 2012, **124**, 4496.

7 A. Abiko, Y. Sy and M. Iguchi, *Polymer*, 2012, **53**, 3842.

8 *Handbook of Ring-Opening Polymerization*, ed. P. Dubois, O. Coulembier and J.-M. Raquez, Wiley-VCH, Weinheim, 2009.

9 (*a*) A. Michalski, M. Brzezinski, G. Lapienis and T. Biela, *Prog. Polym. Sci.*, 2019, **89**, 159; (*b*) J. M. Ren, T. G. McKenzie, Q. Fu, E. H. H. Wong, J. Xu, Z. An, S. Shanmugam, T. P. Davis, C. Boyer and G.-G. Qiao, *Chem. Rev.*, 2016, **116**, 6743.

10 K. Karidi, P. Pladis and C. Kiparissides, *Macromol. Symp.*, 2013, **333**, 206.

11 (*a*) M. Trollsas, B. Atthoff, H. Claesson and J. L. Hedrick, *J. Polym. Sci., Part A: Polym. Chem.*, 2004, **42**, 1174; (*b*) C. M. Dong, K. Y. Qiu, Z. W. Gu and X. D. Feng, *J. Polym. Sci., Part A: Polym. Chem.*, 2001, **40**, 409; (*c*) C. Gottschalk, F. Wolf and H. Frey, *Macromol. Chem. Phys.*, 2007, **208**, 1657; (*d*) L. Wang and C. M. Dong, *J. Polym. Sci., Part A: Polym. Chem.*, 2006, **44**, 2226.

12 (*a*) A. Finne and A. C. Albertsson, *Biomacromolecules*, 2002, **3**, 684; (*b*) K. Odelius, A. Finne and A. C. Albertsson, *J. Polym. Sci., Part A: Polym. Chem.*, 2005, **44**, 596; (*c*) J. Geschwind, S. Rathi, C. Tonhauser, M. Schoemer, S. L. Hsu and E. B. Coughlin, *Macromol. Chem. Phys.*, 2013, **214**, 1434; (*d*) K. Odelius and A. C. Albertsson, *J. Polym. Sci., Part A: Polym. Chem.*, 2008, **46**, 1249; (*e*) H. R. Kricheldorf, *Biomacromolecules*, 2002, **3**, 691; (*f*) H. R. Kricheldorf and B. Fechner, *J. Polym. Sci., Part A: Polym. Chem.*, 2002, **40**, 1047.

13 A. Finne and A. C. Albertsson, *J. Polym. Sci., Part A: Polym. Chem.*, 2003, **41**, 1296.

14 C. A. P. Joziasse, H. Veenstra, M. D. C. Topp, D. W. Grijpma and A. J. Pennings, *Polymer*, 1998, **39**, 467.

15 S. H. Kim, Y. K. Han, Y. H. Kim and S. I. Hong, *Makromol. Chem.*, 1992, **193**, 1623.

16 K. A. George, F. Schue, T. V. Chirila and E. Wentrup-Byrne, *J. Polym. Sci., Part A: Polym. Chem.*, 2009, **47**, 4736.

17 (*a*) Y. Lemmouchi, M. C. Perry, A. J. Amass, K. Chakraborty and E. Schacht, *J. Polym. Sci., Part A: Polym. Chem.*, 2007, **45**, 3966; (*b*) Y. Lemmouchi, M. C. Perry, A. J. Amass,

K. Chakraborty and E. Schacht, *J. Polym. Sci., Part A: Polym. Chem.*, 2008, **6**, 5363.

18 (*a*) H. R. Kricheldorf, H. Hachmann-Thiessen and G. Schwarz, *Biomacromolecules*, 2004, **5**, 492; (*b*) S. Malberg, D. Basalp, A. Finne-Wistrand and A. C. Albertsson, *J. Polym. Sci., Part A: Polym. Chem.*, 2010, **48**, 1214.

19 M. P. Shaver and D. J. A. Cameron, *Biomacromolecules*, 2010, **11**, 3673.

20 M. J. Stanford and A. P. Dove, *Macromolecules*, 2009, **42**, 141.

21 (*a*) C. Hiemstra, Z. Zhong, L. Li, P. J. Dijkstra and J. Feijen, *Biomacromolecules*, 2006, **7**, 2790; (*b*) C. Hiemstra, W. Zhou, Z. Zhong, M. Wouters and J. Feijen, *J. Am. Chem. Soc.*, 2007, **129**, 9918; (*c*) R. Omar, M. Shaik, Ch. Griggs, J. D. Jensen, R. Boyd, N. Oncel, D. C. Webster and G. Du, *Eur. Polym. J.*, 2021, **160**, 110756.

22 W. Guerin, M. Helou, J. F. Carpentier, M. Slawinski, J. M. Brusson and S. M. Guillaume, *Polym. Chem.*, 2013, **4**, 1095.

23 M. P. Shaver and D. J. A. Cameron, *Biomacromolecules*, 2010, **11**, 3673.

24 M. Novák, J. Turek, Y. Milasheuskaya, Z. Růžičková, Š. Podzimek and R. Jambor, *Dalton Trans.*, 2021, **50**, 16039.

25 (*a*) Y. Milasheuskaya, J. Schwarz, L. Dostál, Z. Růžičková, M. Bouška, Z. Olmrová Zmrhalová, T. Syrový and R. Jambor, *Dalton Trans.*, 2021, **50**, 18164; (*b*) M. Kořenková, B. Mairychová, A. Růžička, R. Jambor and L. Dostál, *Dalton Trans.*, 2014, **43**, 7096.

26 X. Li, B. Li, Y. Li and J. Sun, *Chem. Eng. J.*, 2021, **404**, 126504.

27 D. J. Darensbourg and W.-Ch. Chung, *Polyhedron*, 2013, **58**, 139.

28 B. H. Zimm and W. H. Stockmayer, *J. Chem. Phys.*, 1949, **17**, 1301.

29 B. H. Zimm and R. W. Kilb, *J. Polym. Sci.*, 1959, **37**, 19.

30 (*a*) J. Douglas, J. Roovers and K. Freed, *Macromolecules*, 1990, **23**, 4168; (*b*) Note that the *f* calculated this way represent an average value for the entire sample in which different molecules can differ in the number of arms.

31 (*a*) H. Kimura and A. Miyazaki, *Mater. Res. Bull.*, 2001, **36**, 1847; (*b*) A. Prabhakar Reddy, M. Chandrashekhar Reddy, A. Siva Sesha Reddy, J. Ashok, N. Veeraiah and B. Appa Rao, *Appl. Phys. A*, 2018, **124**, 755.